



Research article

Deep learning-based coronary artery calcium score to predict coronary artery disease in type 2 diabetes mellitus

Jingcheng Hu ^{a,1}, Guangyu Hao ^{b,1}, Jialiang Xu ^c, Ximing Wang ^b, Meng Chen ^{b,*}

^a Department of Endocrinology, The First Affiliated Hospital of Soochow University, Suzhou, Jiangsu, China

^b Department of Radiology, The First Affiliated Hospital of Soochow University, Suzhou, Jiangsu, China

^c Department of Cardiology, The First Affiliated Hospital of Soochow University, Suzhou, Jiangsu, China

ARTICLE INFO

Keywords:

Deep learning
Coronary artery calcium score
Coronary artery disease
Type 2 diabetes mellitus
Prediction

ABSTRACT

Background: Coronary artery disease (CAD) in type 2 diabetes mellitus (T2DM) patients often presents diffuse lesions, with extensive calcification, and it is time-consuming to measure coronary artery calcium score (CACS).

Objectives: To explore the predictive ability of deep learning (DL)-based CACS for obstructive CAD and hemodynamically significant CAD in T2DM.

Methods: 469 T2DM patients suspected of CAD who accepted CACS scan and coronary CT angiography between January 2013 and December 2020 were enrolled. Obstructive CAD was defined as diameter stenosis $\geq 50\%$. Hemodynamically significant CAD was defined as CT-derived fractional flow reserve ≤ 0.8 . CACS was calculated with a fully automated method based on DL algorithm. Logistic regression was applied to determine the independent predictors. The predictive performance was evaluated with area under receiver operating characteristic curve (AUC).

Results: DL-CACS (adjusted odds ratio (OR): 1.005; 95% CI: 1.003–1.006; $P < 0.001$) was significantly associated with obstructive CAD. DL-CACS (adjusted OR: 1.003; 95% CI: 1.002–1.004; $P < 0.001$) was also an independent predictor for hemodynamically significant CAD. The AUCs, sensitivities, specificities, positive predictive values and negative predictive values of DL-CACS for obstructive CAD and hemodynamically significant CAD were 0.753 (95% CI: 0.712–0.792), 75.9%, 66.5%, 74.8%, 67.8% and 0.769 (95% CI: 0.728–0.806), 80.7%, 62.1%, 59.6% and 82.3% respectively. It took 1.17 min to perform automated measurement of DL-CACS in total, which was significantly less than manual measurement of 1.73 min ($P < 0.001$).

Conclusions: DL-CACS, with less time-consuming, can accurately and effectively predict obstructive CAD and hemodynamically significant CAD in T2DM.

1. Introduction

The increasing numbers of type 2 diabetes mellitus (T2DM), is a leading cause of disability and mortality, which poses focus on heightened coronary artery disease (CAD) [1]. Comorbidities of hyperglycemia, insulin resistance and hyperlipidemia in T2DM, have synergistically promoted the development and progression of CAD [2], and therefore patients with T2DM have higher incidence of CAD compared with the nondiabetic population [3]. Increase advanced glycation end products (AGEs) increase oxidative stress and

* Corresponding author.

E-mail address: chenmeng9595@126.com (M. Chen).

¹ Jingcheng Hu and Guangyu Hao contributed equally to this work.

activate intracellular signal, which contribute to vascular inflammation, endothelial disfunction injury, vascular smooth muscle cells proliferation and platelet activity [4]. Multiple mechanisms promote vascular calcification through the release of osteoprogenitor cells from marrow into circulation [5], so CAD in T2DM patients often presents with multivessel disease, diffuse lesions, extensive calcification and heavy plaque burden [6]. Addition of obstructive CAD to traditional model improved the prediction of major adverse cardiovascular events (MACE) in asymptomatic T2DM patients [7]. Patient with hemodynamically significant CAD was associated with a high incidence of MACE [8]. Therefore, predictions for obstructive CAD and hemodynamically significant CAD in T2DM can provide prognostic information and optimize downstream risk management.

With the advantages of high sensitivity, non-invasion and easy accessibility, coronary artery calcium score (CACS) has been widely applied to assess CAD in T2DM patients. However manual measurement of CACS is time-consuming in T2DM patients with diffuse calcification. Research revealed that deep learning-based CACS (DL-CACS) exhibited great application value in medical imaging, and automated evaluation improved the efficiency, repeatability and objectivity of measurement [9]. Therefore, this study aimed to explore the predictive values of DL-CACS for obstructive CAD and hemodynamically significant CAD in T2DM patients.

2. Material and methods

2.1. Study population

Institutional ethics review board approval was obtained in this study (NO. 2020-256) and written informed consent was waived because of the retrospective research design, however informed consents were acquired from the patients for the publication of their images. T2DM patients suspected of CAD who accepted CACS scan and coronary computed tomography angiography (CCTA) between January 2013 and December 2020 were enrolled, with clinical factors, plaque parameters and revascularization therapies [percutaneous coronary intervention (PCI) and coronary artery bypass grafting (CABG)] within 3 months after CCTA collected. The exclusion criteria in this research were shown in Fig. 1.

Diagnostic criteria of T2DM was in accord with the guideline [10]. Clinical risk factors, in the aspects of age, sex, body mass index, hypertension, hyperlipidemia and smoker/drinker, were obtained from medical records. Additionally, total cholesterol (TC), triglyceride (TG), high-density lipoprotein cholesterol, low-density lipoprotein cholesterol, Apolipoprotein A (ApoA), Apolipoprotein B (ApoB), lipoprotein (a), fasting blood-glucose, glycosylated hemoglobin (HbA1c), high-sensitivity C-reactive protein, systolic blood pressure (SBP) and diastolic blood pressure (DBP) at baseline were collected. Hyperlipidemia was considered as serum TG \geq 200 mg/dl or TC \geq 230 mg/dl or taking antihyperlipidemic drugs. Hypertension was defined as SBP \geq 140 mmHg or DBP \geq 90 mmHg or taking antihypertensive drugs. Smoker/drinker was defined as having a history of smoking/drinking at present or in the past one year. Medications were also collected consecutively, including oral hypoglycemic agents, insulin, statin and antihypertensive drugs.

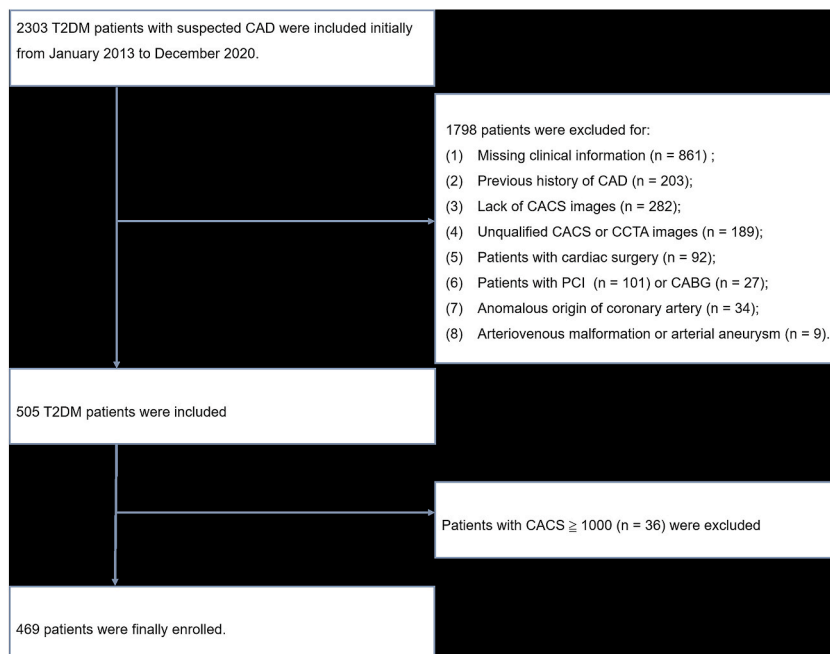


Fig. 1. Flow chart.

2.2. CT protocols

Image acquisitions were performed using 2 different vendors (Somatom Flash, Siemens Healthineers, Germany; Revolution CT, GE Healthcare, USA). Patients with heart rate ≥ 70 beats/min were given oral beta-blockers. Each patient received sublingual nitroglycerin before electrocardiograph (ECG)-triggered CACS scan and CCTA scan. The region of interest was located in the ascending aorta and a bolus-tracking technology was used, with contrast media (Ultravist, Bayer, Germany; Iodixanol, Nycomed, Norway) administered. Detailed scan parameters were displayed in [Supplementary Table 1](#).

Iterative reconstruction was applied to reconstruct CCTA images, with ECG editing used if necessary, and CCTA analysis used the phase with the optimal image quality.

2.3. Automated and manual measurement of CACS

A fully automated software (CACScoreDoc, ShuKun Network Technology, Beijing) was employed for CACS calculation based on DL algorithm. As described in previous study [9], the CACS images were transformed into three-dimensional (3D) volume data first. Then, all the voxel points were divided with a CT value ≥ 130 Hounsfield unit (HU) and the connected regions in the volume were marked as they were suspected of the calcified regions. Coronary artery calcium lesions were segmented by cascaded modified 3D U-Net DL models [11] and divided into: left main stem calcium, left anterior descending calcium, left circumflex calcium and right coronary artery calcium. Then, the image segmentation results were based to calculate total DL-CACS (Fig. 2). Finally, radiologist confirmed the results calculated by the software and manual modification could be performed if there existed any incorrect identification of calcified regions. Total DL-CACS was divided into four groups: 0, 1–99, 100–299 and 300–999 [12].

CACS images were transferred to the advanced workstations (syngo.via v. 4.1, Siemens Healthcare; Advantage workstation v. 4.7, GE healthcare) for manual analysis. The CACS was computed if the CT attenuation ≥ 130 HU [13]. The computation of manual CACS was determined by the weighted density score given to the highest CT value (HU) multiplied by the calcified areas. Total manual CACS was acquired by adding the scores of every coronary artery. Radiology with 10 years of experience in CCTA diagnosis independently delineated the calcified regions and calculated the CACS in 100 randomly selected patients.

2.4. Plaque analysis in CCTA images

Dedicated software (CoronaryDoc, ShuKun Network Technology, Beijing) embedded with DL algorithm was utilized to process CCTA images for vessel extraction and image post-processing [14]. Two radiologists (9 and 10 years of experience in CCTA diagnosis) who were ignorant about patient information assessed the diameter stenosis (DS), high-risk plaque (HRP), multi-vessel coronary artery disease (MVD) independently on patient-based analysis. Any discrepancy was resolved in consensus with senior radiologist with 20 years of experience. DS was classified into: no visible stenosis, minimal stenosis, mild stenosis, moderate stenosis, severe stenoses and occluded [15]. Obstructive CAD was identified as DS $\geq 50\%$ in CCTA. MVD was identified as DS $\geq 50\%$ by visual evaluation in two or more major coronary arteries or side branches [16]. HRP features were defined as spotty calcification, low attenuation, napkin ring sign and positive remodeling [17]. If two or more HRP features were satisfied, HRP was considered to be positive [15].

2.5. CCTA derived fractional flow reserve (CT-FFR) analysis

CT-FFR calculations were performed using CCTA datasets in dedicated software (DEEPVESSEL-FFR, Keya Medical) as previously described [18]. The DL framework included multilayer neural network (MLNN) and bi-directional recursive neural network (BRNN). The MLNN with three fully connected layers took the anatomical structure along coronary artery trees as the input, including lesion characteristics and proximal/distal markers defined for each lesion. The fully connected layers transformed input characteristics into features with weight Vs, which were received by BRNN. First, a 3D coronary artery tree and its centerlines were extracted for a given

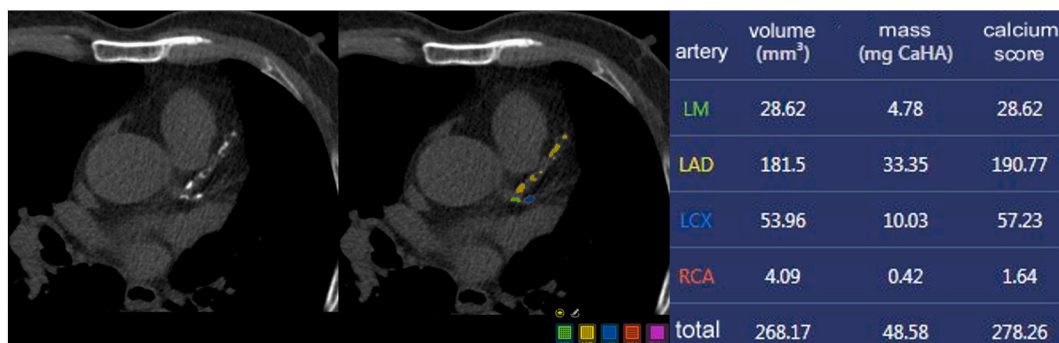


Fig. 2. Automated identification of calcified regions in coronary arteries and results presentation of DL-CACS. DL-CACS, deep learning-based coronary artery calcium score.

CCTA image. Subsequently CT-FFR values were determined along these centerlines with the MLNN-BRNN. The CT-FFR values were calculated at the 2 cm distal to each lesion and CT-FFR ≤ 0.8 was defined as hemodynamically significant CAD.

2.6. Intra-observer and inter-observer agreement

Intra-observer and inter-observer variabilities for DL-CACS, DS, HRP and MVD were conducted respectively among 50 random patients. The same observer evaluated the parameters with the time interval of 1 month or above in order to eliminate recall bias.

Table 1
Clinical characteristics.

Characteristics	Total cohorts (n = 469)	Obstructive CAD			Hemodynamically significant CAD		
		Positive cohort (n = 266)	Negative cohort (n = 203)	P	Positive cohort (n = 192)	Negative cohort (n = 277)	P
Age (years)	64 (56, 70)	64 (58, 72)	62 (54, 69)	0.012*	64 (58, 71)	62 (54, 69)	0.031*
Male	289 (61.6)	198 (74.4)	91 (44.8)	< 0.001*	150 (78.1)	139 (50.2)	< 0.001*
Body mass index (kg/m ²)	24.30 (22.65, 26.75)	24.20 (22.68, 26.53)	24.40 (22.50, 27.00)	0.639	24.20 (22.53, 25.98)	24.40 (22.70, 27.40)	0.095
Smoker	140 (29.9)	98 (36.8)	42 (20.7)	< 0.001*	77 (40.1)	63 (22.7)	< 0.001*
Drinker	91 (19.4)	65 (24.4)	26 (12.8)	0.002*	44 (22.9)	47 (17.0)	0.109
Hyperlipidemia	240 (51.2)	142 (53.4)	98 (48.3)	0.273	103 (53.6)	137 (49.5)	0.372
Hypertension	366 (78.0)	211 (79.3)	155 (76.4)	0.442	152 (79.2)	214 (77.3)	0.623
Systolic blood pressure (mmHg)	135 (123, 150)	134 (120, 148)	137 (124, 150)	0.231	135 (120, 148)	135 (124, 150)	0.466
Diastolic blood pressure (mmHg)	80 (73, 87)	80 (72, 87)	80 (75, 88)	0.183	80 (71, 86)	80 (74, 88)	0.105
Duration of diabetes (years)	5 (2, 10)	6 (2, 14)	5 (2, 10)	0.184	6 (2, 15)	5 (2, 10)	0.030*
Laboratory tests							
Fast glucose (mmol/L)	6.88 (5.87, 8.46)	6.96 (5.91, 8.67)	6.81 (5.71, 8.22)	0.287	6.88 (5.90, 8.45)	6.89 (5.83, 8.47)	0.806
HbA1c (%)	7.20 (6.50, 8.50)	7.50 (6.60, 8.90)	6.80 (6.20, 7.70)	< 0.001*	7.50 (6.60, 9.00)	7.10 (6.40, 7.90)	< 0.001*
Total cholesterol (mmol/L)	4.30 (3.64, 5.17)	4.17 (3.56, 5.02)	4.51 (3.82, 5.34)	0.009*	4.27 (3.69, 5.07)	4.30 (3.63, 5.21)	0.653
Triglycerides (mmol/L)	1.47 (1.06, 2.24)	1.45 (1.07, 2.15)	1.52 (1.05, 2.39)	0.450	1.38 (1.09, 2.15)	1.52 (1.04, 2.36)	0.428
HDL-C (mmol/L)	1.06 (0.91, 1.27)	1.04 (0.90, 1.22)	1.07 (0.92, 1.29)	0.086	1.06 (0.90, 1.23)	1.06 (0.91, 1.28)	0.587
LDL-C (mmol/L)	2.42 (1.87, 3.33)	2.40 (1.83, 3.24)	2.55 (1.93, 3.35)	0.244	2.46 (1.91, 3.33)	2.40 (1.85, 3.31)	0.428
Hs-CRP (mg/L)	1.58 (0.73, 3.64)	1.58 (0.69, 3.38)	1.58 (0.73, 4.39)	0.597	1.56 (0.68, 3.33)	1.70 (0.74, 4.25)	0.427
DL-CACS	78.18 (1.49, 256.89)	150.94 (48.13, 364.09)	9.33 (0.00, 90.60)	< 0.001*	232.74 (74.17, 450.58)	18.96 (0.00, 114.19)	< 0.001*
Categorical DL-CACS							
0	108 (23.0)	31 (11.7)	77 (37.9)	< 0.001*	17 (8.9)	91 (32.9)	< 0.001*
1-99	157 (33.5)	77 (28.9)	80 (39.4)		47 (24.5)	110 (39.7)	
100-299	103 (22.0)	71 (26.7)	32 (15.8)		53 (27.6)	50 (18.1)	
300-999	101 (21.5)	87 (32.7)	14 (6.9)		75 (39.1)	26 (9.4)	
Revascularization therapy	82 (17.5)	80 (30.1)	2 (1.0)	< 0.001*	68 (35.4)	14 (5.1)	< 0.001*
PCI	79 (16.8)	77 (28.9)	2 (1.0)		65 (33.9)	14 (5.1)	
CABG	3 (0.6)	3 (1.1)	0 (0.0)		3 (1.6)	0 (0.0)	
Medication compliance							
Oral hypoglycemic agents	403 (85.9)	233 (87.6)	170 (83.7)	0.235	171 (89.1)	232 (83.8)	0.104
Insulin	67 (14.3)	47 (17.7)	20 (9.9)	0.017*	36 (18.8)	31 (11.2)	0.021*
Statin	116 (24.7)	78 (29.3)	38 (18.7)	0.008*	58 (30.2)	58 (20.9)	0.022*
Antihypertensive drugs	335 (71.4)	196 (73.7)	139 (68.5)	0.216	143 (74.5)	192 (69.3)	0.223

CAD, coronary artery disease; HbA1c, glycosylated hemoglobin; HDL-C, high-density lipoprotein cholesterol; LDL-C, low-density lipoprotein cholesterol; hs-CRP, high-sensitivity C-reactive protein; DL-CACS, deep learning-based coronary artery calcium score; PCI, percutaneous coronary intervention; CABG, coronary artery bypass grafting.

2.7. Statistical analysis

Statistical analysis was performed with SPSS Statistics (v. 26.0, IBM Corp, Armonk, NY, USA), R environment (R version 4.05 and R Studio version 4.0), PASS software (version 15.0.5, Kaysville, Utah, USA), and MedCalc Software (v. 19.6.4, Ostend, Belgium). Power analyses for receiver operating characteristic (ROC) curves were performed with PASS software. A two-sided $P < 0.05$ was deemed to be statistically significant. Overall, 16.3% of observations were missing, and continuous variables were imputed using multiple imputation. Five imputations were carried out with “mice” package and the imputation data with the least Akaike Information criterion (AIC) was selected for subsequent statistical analysis. The variables with missing rate $\geq 50\%$ were deleted, including ApoA, ApoB, lipoprotein (a).

Continuous data were recorded as means \pm standard deviations or median and quartile (Q1, Q3) according to the distributions (One-sample Kolmogorov-Smirnov test). Independent-sample t -test was used to analyze data with normal distribution, while Mann-Whitney U test was performed conversely. Categorical variables were expressed as count (%) and compared with chi-square test, while differences in CAD, HRP and revascularization therapy among different categorical DL-CACS were analyzed with chi-square test for trend. The agreement between DL-CACS and manual CACS was evaluated with intraclass correlation coefficient (ICC). The intra- and inter-observer agreements of DL-CACS, DS, HRP and MVD were assessed by ICC or Kappa statistic.

Clinical risk factors, DL-CACS and plaque features were filtered first by univariate logistic regression. Variables with $P < 0.1$ were integrated into multivariate logistic regression, and subsequently significant variables with $P < 0.05$ in multivariate logistic regression were independent predictors with the odds ratio (OR) and 95% confidence interval (CI) calculated. Predictive performance was determined by the area under curve (AUC) of ROC. Sensitivity, specificity, positive predictive value (PPV) and negative predictive value (NPV) were calculated according to the maximum Youden index.

3. Results

3.1. Clinical characteristics

Totally, 469 T2DM patients with suspected CAD were included finally (Fig. 1). There were 289 males and 180 females, with the median age of 64 (56, 70) years. There were 266 patients with obstructive CAD and 192 patients with hemodynamically significant CAD. Power analyses of DL-CACS for both obstructive CAD and hemodynamically significant CAD showed adequate statistical power (both power = 1.00). The detailed clinical characteristics at baseline were shown in Table 1. Electrolyte data, liver and kidney function tests were demonstrated in Supplementary Table 2.

In comparison with patients without obstructive CAD, patients with obstructive CAD had higher age, HbA1c and DL-CACS. Patients with obstructive CAD showed higher proportions of male, smoker, drinker, revascularization therapy, insulin use and statin use than patients without obstructive CAD. The level of TC in patients with obstructive CAD was significantly lower, which might be related with higher percentage of statin use. Patients with hemodynamically significant CAD had higher age, duration of T2DM, HbA1c and DL-CACS and higher proportions of male, smoker, revascularization therapy, insulin use and statin use than patients without hemodynamically significant CAD.

3.2. The comparison between DL-CACS and manual CACS

There was no difference between DL-CACS [122.26 (5.01, 417.66)] and manual CACS [114.19 (4.18, 398.43)], and the ICC was 0.961 (95% CI: 0.943–0.974; $P < 0.001$).

3.3. Reproducibility analysis

Good or excellent intra-observer and inter-observer reliabilities for DL-CACS, DS, HRP and MVD assessment were shown in Supplementary Table 3.

3.4. Differences in CAD, HRP and revascularization therapy among different categorical DL-CACS

The proportions of obstructive CAD, hemodynamically significant CAD and revascularization therapy increased gradually with

Table 2
Differences in CAD, HRP and revascularization among different categorical DL-CACS.

Categorical DL-CACS	Obstructive CAD [n (%)]	Hemodynamically significant CAD [n (%)]	High-risk plaque [n (%)]	Revascularization [n (%)]
0	31 (28.7)	17 (15.7)	22 (20.4)	6 (5.6)
1–99	77 (49.0)	47 (29.9)	56 (35.7)	23 (14.6)
100–299	71 (68.9)	53 (51.5)	48 (46.6)	26 (25.2)
300–999	87 (86.1)	75 (74.3)	42 (41.6)	27 (26.8)
P for trend	< 0.001	< 0.001	< 0.001	< 0.001

DL-CACS, deep learning-based coronary artery calcium score; CAD, coronary artery disease.

increased categorical DL-CACS (All P for trend < 0.001 , Table 2). With the increase of categorical DL-CACS, the proportion of HRP increased gradually, however there existed slight decrease when DL-CACS was above 300 (P for trend < 0.001).

3.5. Predictive performance of DL-CACS for obstructive CAD

Univariate and multivariable logistic regression showed DL-CACS (adjusted OR: 1.005; $P < 0.001$), age (adjusted OR: 1.034; $P = 0.004$), male (adjusted OR: 3.766; $P < 0.001$), smoker (adjusted OR: 1.723; $P = 0.048$) and HbA1c (adjusted OR: 1.313; $P < 0.001$) were significantly associated with obstructive CAD (Table 3). The AUC, sensitivity, specificity, PPV and NPV of DL-CACS for obstructive CAD were 0.753 (95% CI: 0.712–0.792), 75.9%, 66.5%, 74.8% and 67.8% respectively (Fig. 3A).

3.6. Predictive performance of DL-CACS for hemodynamically significant CAD

Univariate and multivariable logistic regression showed DL-CACS (adjusted OR: 1.003; $P < 0.001$), male (adjusted OR: 2.275; $P = 0.004$), BMI (adjusted OR: 0.900; $P = 0.013$), obstructive CAD (adjusted OR: 5.876; $P < 0.001$), MVD (adjusted OR: 4.098; $P < 0.001$) and HRP (adjusted OR: 2.093; $P = 0.007$) were recognized as independent predictors for hemodynamically significant CAD (Table 4). The AUC, sensitivity, specificity, PPV and NPV of DL-CACS for hemodynamically significant CAD were 0.769 (95% CI: 0.728–0.806), 80.7%, 62.1%, 59.6% and 82.3% respectively (Fig. 3B). Fig. 4 (A–D) demonstrated a representative case.

3.7. Time comparison between DL-CACS and manual CACS

Median time of DL-CACS was 1.17 (1.08, 1.25) minutes, including automated calculation time of 0.88 (0.83, 0.93) minute and doctor's confirmation time of 0.27 (0.20, 0.37) minute, which was significantly less than manual measurement time of 1.73 (1.48, 2.26) minutes ($Z = -9.665$; $P < 0.001$).

4. Discussion

In this study, DL-CACS, with fast and reliable calculation, could be used for predictions of obstructive CAD and hemodynamically significant CAD in T2DM patients, which showed wide prospect in clinical application.

Finding new and efficient method to predict high-risk CAD is vital importance, as unique factors in T2DM patients increase atherosclerotic plaque and thrombosis, thereby leading to myocardial infarction [19], so early detection of high-risk CAD patients with MACE risk can offer opportunity for early intervention and therapy. The study demonstrated that DL-CACS was associated with obstructive CAD and hemodynamically significant CAD, and showed accurate predictive ability. The proportions of CAD, HRP and revascularization therapy increased gradually with increased categorical DL-CACS, indicating DL-CACS could reflect the risk and severity of CAD in T2DM. Currently, it remains highly controversial to screen asymptomatic CAD with CCTA in T2DM patients [20,21]: relative low incidence and cardiac event rate, expensive cost and radiation exposure. With the advantages of good discrimination, low cost and low radiation dose, DL-CACS serves as a specific predictor for symptomatic CAD [22] and is also a risk stratification and management tool for asymptomatic CAD in T2DM patients [23]. Besides, the research [11] indicated it was achievable to acquire DL-CACS based on non-gated chest CT image within a short time without adding radiation dose or extra economic cost, which showed good clinical universality and might be a potential evaluation tool for CAD in T2DM patients.

The diffuse calcification of coronary arteries in T2DM posed challenges for manual measurement of CACS, which took a relatively long time. In this study, DL-CACS could overcome the above deficiencies and achieved stable and reliable results. The automated calculation time of DL was less than 1 min and the doctor's confirmation time was less than half a minute, which showed excellent prospect in clinical application. The agreement of DL-CACS and manual CACS was in accord with previous study [24]. The ICC of DL-CACS and manual CACS was better than previous study (0.96 vs. 0.94), which was related with doctor's confirmation on the basis of DL. Although fully automated calculation was fast and didn't occupy doctor's time, there existed rare cases of wrong identification of calcified regions, such as calcifications of the aortic sinus, mitral valve and left hilum adjacent to the left circumflex calcium, so doctor's confirmation could further improve the accuracy.

Table 3
Univariate and multivariate logistic regression of variables for obstructive CAD.

Variable	Univariate		Multivariate	
	OR (95% CI)	P	OR (95% CI)	P
Age	1.025 (1.007–1.043)	0.007	1.034 (1.011–1.058)	0.004
Male	3.584 (2.425–5.295)	< 0.001	3.766 (2.270–6.247)	< 0.001
Smoker	2.236 (1.468–3.407)	< 0.001	1.723 (1.005–2.954)	0.048
Drinker	2.201 (1.338–3.621)	0.002		0.305
Insulin	1.964 (1.123–3.434)	0.018		0.983
TC	0.865 (0.743–1.006)	0.060		0.374
HbA1c	1.304 (1.155–1.473)	< 0.001	1.313 (1.146–1.503)	< 0.001
DL-CACS	1.005 (1.004–1.007)	< 0.001	1.005 (1.003–1.006)	< 0.001

CAD, coronary artery disease; TC, total cholesterol; HbA1c, glycosylated hemoglobin; DL-CACS, deep learning-based coronary artery calcium score.

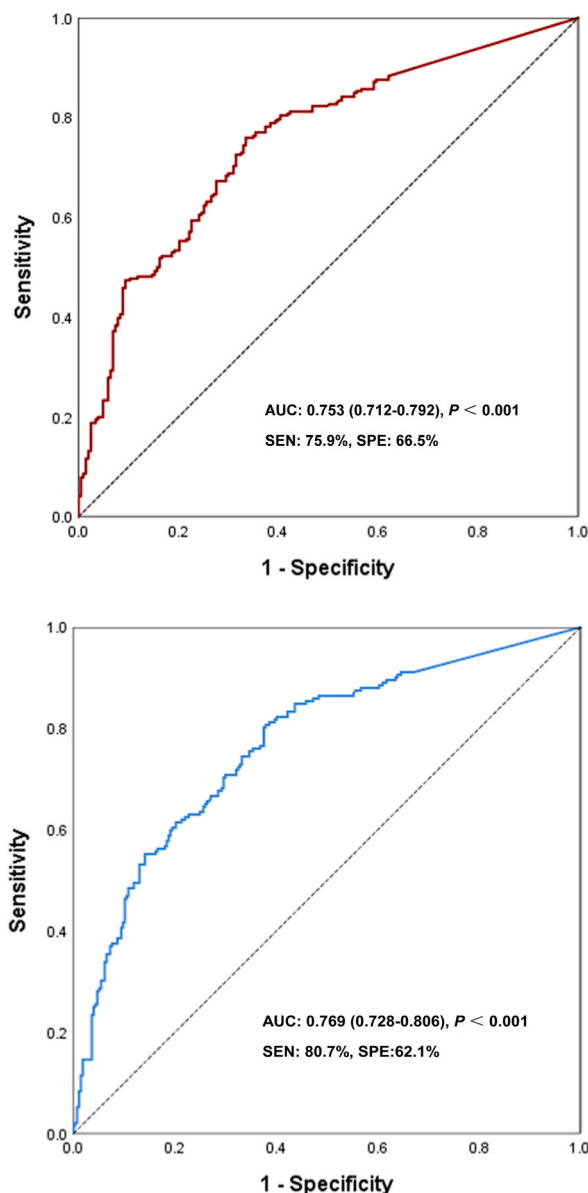


Fig. 3. ROC curves of DL-CACS for obstructive CAD (AUC: 0.753, 3A) and hemodynamically significant CAD (AUC: 0.769, 3B). ROC, receiver operating characteristic; DL-CACS, deep learning-based coronary artery calcium score; CAD, coronary artery disease; AUC, area under ROC curve.

Prediction of obstructive CAD with CCAT as reference standard was more representative than that with invasive coronary angiography (ICA) as golden standard, because high positive rate of obstructive CAD in the patients who accepted ICA might lead to selection bias. Consistent with previous study [25], DL-CACS accurately estimated the pretest likelihood of obstructive CAD, but the AUC was lower than previous study (AUC: 0.753 vs. 0.819) [22], which might be related with the below reasons. First, diffuse coronary calcification in T2DM had influence on the DS assessment, especially for the intermediate lesion approaching 50% stenosis. Second, relatively high positive rate of obstructive CAD (56.7%) might be one reason of low specificity and NPV. Third, patients with CACS ≥ 1000 were excluded in this study, out of concern for high false positive rate resulted from massive calcification in DS assessment, which led to the decreased AUC because increased CACS was associated with high incidence of CAD. In addition, it was controversial whether massive calcification had effect on the accuracy of CT-FFR [26,27]. Researches pointed out high CACS (> 1000) affected the accuracy of CT-FFR [28], especially for the specificity [26]. DL-CACS showed excellent sensitivity to detect hemodynamically significant CAD. Meanwhile, high NPV of DL-CACS demonstrated an effective alternative to rule out hemodynamically significant CAD.

Patients with obstructive CAD and hemodynamically significant CAD had higher proportions of insulin use and insulin use was associated with obstructive CAD and hemodynamically significant CAD in univariate logistic regression, which might be mostly due to the fact that patients with consecutive insulin use had worse pancreatic beta cell functionality and viability and had more difficulty in

Table 4
Univariate and multivariate logistic regression of variables for hemodynamically significant CAD.

Variable	Univariate		Multivariate	
	OR (95% CI)	P	OR (95% CI)	P
Age	1.021 (1.003–1.040)	0.024		0.821
Male	3.546 (2.340–5.372)	< 0.001	2.275 (1.291–4.012)	0.004
BMI	0.929 (0.877–0.984)	0.012	0.900 (0.829–0.978)	0.013
Smoker	2.274 (1.520–3.402)	< 0.001		0.170
Duration of T2DM	1.026 (0.999–1.053)	0.055		0.423
Insulin	1.831 (1.088–3.082)	0.023		0.844
HbA1c	1.223 (1.097–1.363)	< 0.001		0.510
DL-CACS	1.005 (1.004–1.006)	< 0.001	1.003 (1.002–1.004)	< 0.001
Obstructive CAD	21.041 (12.049–36.743)	< 0.001	5.876 (3.076–11.228)	< 0.001
Multi-vessel disease	16.176 (9.457–27.668)	< 0.001	4.098 (2.193–7.659)	< 0.001
High-risk plaque	4.852 (3.235–7.277)	< 0.001	2.093 (1.223–3.581)	0.007

T2DM, type 2 diabetes mellitus; HbA1c, glycosylated hemoglobin; CAD, coronary artery disease; DL-CACS, deep learning-based coronary artery calcium score.

controlling the blood glucose. In the study, we assumed insulin other treatment for T2DM, because oral hypoglycemic agents, such as Sodium-Glucose Cotransporter-2 Inhibitors (SLGT-2i) or metformin, had direct antioxidant and antiatherosclerotic effects on T2DM patients, followed by promotion in insulin sensitivity, leading to a decrease in cardiovascular complications [29].

The present study had several limitations. Firstly, it was researched retrospectively and therefore prospective research in large cohort studies would be needed further. Meanwhile, screening for asymptomatic CAD in T2DM patients with DL-CACS is beneficial to early treatment and prevention of complication. Secondly, the study was of limited value in patients with T2DM and CAD who had non-calcified plaque only, although the number of this population was relatively small. This subgroup may benefit from annual monitor of CACS because of diffuse calcification of coronary artery during the process. Thirdly, analysis in “gray-zone” patients (CT-FFR value between 0.75 and 0.80) was not allowed because of insufficient sample size. Expanding the sample size is essential to guide the treatment strategy in “gray-zone” patients. Fourthly, the percentage of missing data was relatively high, because many variables were included in the study. Last, we acknowledged that a positive rate of 56.7% obstructive CAD was relatively high, leading to the selection bias.

5. Conclusion

DL-CACS can accurately and effectively predict obstructive CAD and hemodynamically significant CAD in T2DM patients, with less time-consuming, and has broad clinical application prospect.

Data availability statement

The data that has been used is confidential. However, data may be available on a reasonable individual request upon approval of all authors.

Funding

This work was supported by Jiangsu Medical Association [SYH-3201150-0016(2021011)] and Suzhou Municipal Health Commission (GSWS2020003, KJXW2020007).

CRediT authorship contribution statement

Jingcheng Hu: Writing – original draft, Software, Resources, Methodology, Data curation, Conceptualization. **Guangyu Hao:** Writing – original draft, Visualization, Methodology, Investigation, Formal analysis, Data curation, Conceptualization. **Jialiang Xu:** Resources, Methodology, Investigation, Formal analysis. **Ximing Wang:** Supervision, Resources, Project administration, Data curation. **Meng Chen:** Writing – review & editing, Writing – original draft, Validation, Supervision, Software, Resources, Project administration, Methodology, Funding acquisition, Data curation, Conceptualization.

Declaration of competing interest

The authors declare that they have no known competing financial interests or personal relationships that could have appeared to influence the work reported in this paper.

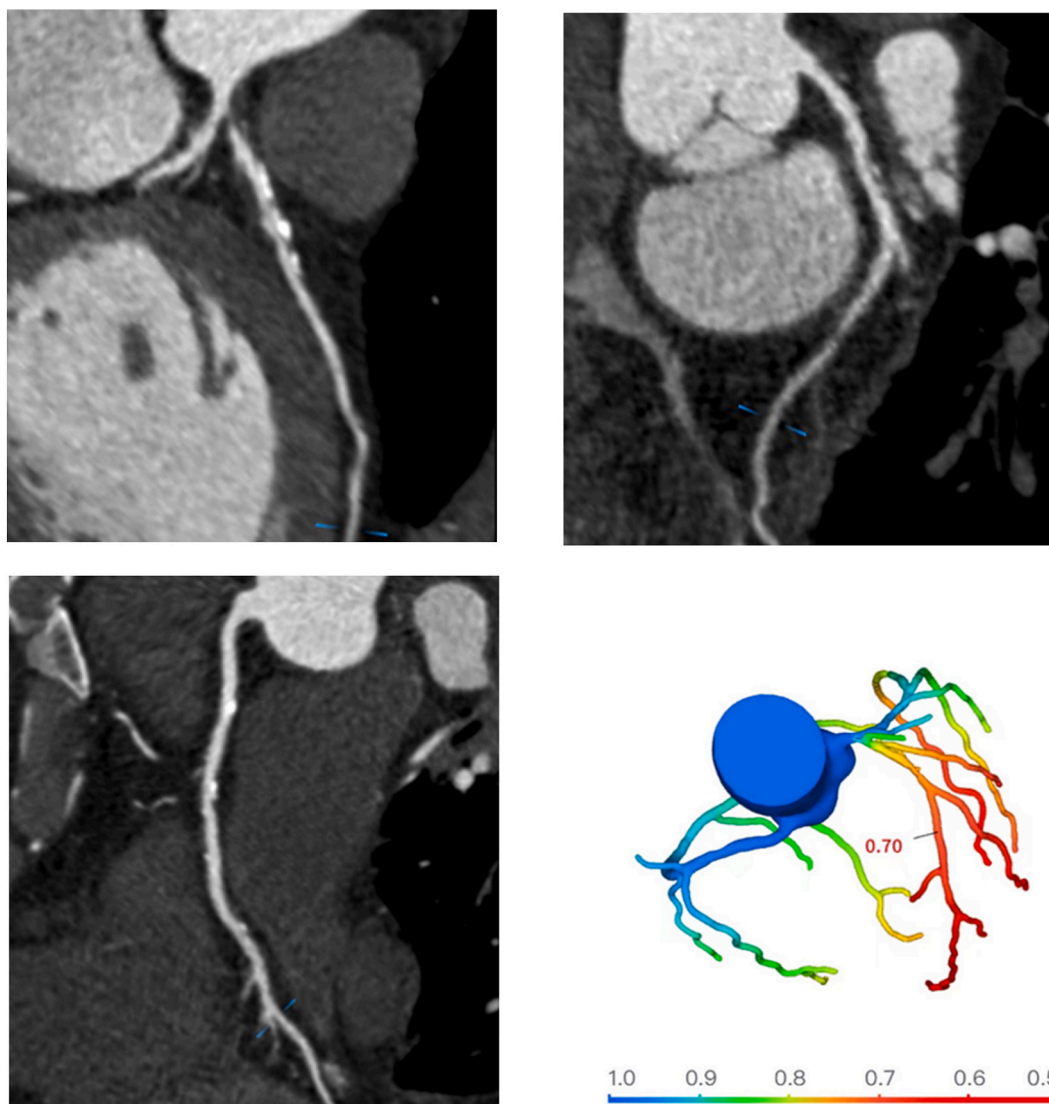


Fig. 4. Representative case of a 64 years old male showed obstructive stenosis (4A: LAD; 4B: LCX; 4C: RCA) and hemodynamically significant stenosis (4D) in LAD and LCX. DL-CACS of the patient was 333.18. CAD, coronary artery disease; LAD, left anterior descending calcium; LCX, left circumflex calcium; RCA, right coronary artery calcium; DL-CACS, deep learning-based coronary artery calcium score.

Appendix A. Supplementary data

Supplementary data to this article can be found online at <https://doi.org/10.1016/j.heliyon.2024.e27937>.

References

- [1] GBD 2017 Disease and Injury Incidence and Prevalence Collaborators, Global, regional, and national incidence, prevalence, and years lived with disability for 354 diseases and injuries for 195 countries and territories, 1990-2017: a systematic analysis for the Global Burden of Disease Study 2017, *Lancet* 392 (2018) 1789–1858, [https://doi.org/10.1016/S0140-6736\(18\)32279-7](https://doi.org/10.1016/S0140-6736(18)32279-7).
- [2] R. Shi, Y. Gao, L.L. Shen, K. Shi, J. Wang, L. Jiang, Y. Li, Z.G. Yang, The effect of LDL-C status on the association between increased coronary artery calcium score and compositional plaque volume progression in statins-treated diabetic patients: evaluated using serial coronary CTAs, *Cardiovasc. Diabetol.* 21 (2022) 121, <https://doi.org/10.1186/s12933-022-01556-y>.
- [3] L.C. Godoy, D.T. Ko, V. Rao, M.E. Farkouh, The role of coronary artery bypass surgery versus percutaneous intervention in patients with diabetes and coronary artery disease, *Prog. Cardiovasc. Dis.* 62 (2019) 358–363, <https://doi.org/10.1016/j.pcad.2019.07.004>.
- [4] M. Kosmopoulos, D. Drekolias, P.D. Zavras, C. Piperi, A.G. Papavassiliou, Impact of advanced glycation end products (AGEs) signaling in coronary artery disease, *Biochim. Biophys. Acta, Mol. Basis Dis.* 1865 (2019) 611–619, <https://doi.org/10.1016/j.bbadis.2019.01.006>.

- [5] K. Yahagi, F.D. Kolodgie, C. Lutter, H. Mori, M.E. Romero, A.V. Finn, R. Virmani, Pathology of human coronary and carotid artery atherosclerosis and vascular calcification in diabetes mellitus, *Arterioscler. Thromb. Vasc. Biol.* 37 (2017) 191–204, <https://doi.org/10.1161/ATVBAHA.116.306256>.
- [6] K. Cui, S. Lyu, H. Liu, X. Song, F. Yuan, F. Xu, M. Zhang, W. Wang, M. Zhang, D. Zhang, J. Tian, Staged complete revascularization or culprit-only percutaneous coronary intervention for multivessel coronary artery disease in patients with ST-segment elevation myocardial infarction and diabetes, *Cardiovasc. Diabetol.* 18 (2019) 119, <https://doi.org/10.1186/s12933-019-0923-0>.
- [7] K.Y. Lee, B.H. Hwang, T.H. Kim, C.J. Kim, J.J. Kim, E.H. Choo, I.J. Choi, Y. Choi, H.W. Park, Y.S. Koh, P.J. Kim, J.M. Lee, M.J. Kim, D.S. Jeon, J.H. Cho, J. I. Jung, K.B. Seung, K. Chang, Computed tomography angiography images of coronary artery stenosis provide a better prediction of risk than traditional risk factors in asymptomatic individuals with type 2 diabetes: a long-term study of clinical outcomes, *Diabetes Care* 40 (2017) 1241–1248, <https://doi.org/10.2337/dc16-1844>.
- [8] B.L. Norgaard, S. Gaur, T.A. Fairbairn, P.S. Douglas, J.M. Jensen, M.R. Patel, A.R. Ithdayhid, B.S.H. Ko, S.L. Sellers, J. Weir-McCall, H. Matsuo, N.P.R. Sand, K. A. Ovrehus, C. Rogers, S. Mullen, K. Nieman, E. Parner, J. Leipsic, J. Abdulla, Prognostic value of coronary computed tomography angiographic derived fractional flow reserve: a systematic review and meta-analysis, *Heart* 108 (2022) 194–202, <https://doi.org/10.1136/heartjnl-2021-319773>.
- [9] W. Wang, H. Wang, Q. Chen, Z. Zhou, R. Wang, H. Wang, N. Zhang, Y. Chen, Z. Sun, L. Xu, Coronary artery calcium score quantification using a deep-learning algorithm, *Clin. Radiol.* 75 (2020) 237 e211–e237 e216, <https://doi.org/10.1016/j.crad.2019.10.012>.
- [10] W. Kerner, J. Bruckel, A. German Diabetes, Definition, classification and diagnosis of diabetes mellitus, *Exp. Clin. Endocrinol. Diabetes* 122 (2014) 384–386, <https://doi.org/10.1055/s-0034-1366278>.
- [11] J. Xu, J. Liu, N. Guo, L. Chen, W. Song, D. Guo, Y. Zhang, Z. Fang, Performance of artificial intelligence-based coronary artery calcium scoring in non-gated chest CT, *Eur. J. Radiol.* 145 (2021) 110034, <https://doi.org/10.1016/j.ejrad.2021.110034>.
- [12] H.S. Hecht, M.J. Blaha, E.A. Kazerooni, R.C. Cury, M. Budoff, J. Leipsic, L. Shaw, CAC-DRS: coronary artery calcium data and reporting system. An expert consensus document of the society of cardiovascular computed tomography (SCCT), *J Cardiovasc Comput Tomogr* 12 (2018) 185–191, <https://doi.org/10.1016/j.jcct.2018.03.008>.
- [13] I.C. Thomas, N.I. Forbang, M.H. Crique, The evolving view of coronary artery calcium and cardiovascular disease risk, *Clin. Cardiol.* 41 (2018) 144–150, <https://doi.org/10.1002/clc.22842>.
- [14] M. Chen, X. Wang, G. Hao, X. Cheng, C. Ma, N. Guo, S. Hu, Q. Tao, F. Yao, C. Hu, Diagnostic performance of deep learning-based vascular extraction and stenosis detection technique for coronary artery disease, *Br. J. Radiol.* 93 (2020) 20191028, <https://doi.org/10.1259/bjr.20191028>.
- [15] R.C. Cury, S. Abbara, S. Achenbach, A. Agatston, D.S. Berman, M.J. Budoff, K.E. Dill, J.E. Jacobs, C.D. Maroules, G.D. Rubin, F.J. Rybicki, U.J. Schoepf, L. J. Shaw, A.E. Stillman, C.S. White, P.K. Woodard, J.A. Leipsic, CAD-RADS(TM) coronary artery disease - reporting and data system. An expert consensus document of the society of cardiovascular computed tomography (SCCT), the American college of radiology (ACR) and the North American Society for cardiovascular imaging (NASCI). Endorsed by the American College of Cardiology, *J Cardiovasc Comput Tomogr* 10 (2016) 269–281, <https://doi.org/10.1016/j.jcct.2016.04.005>.
- [16] A.A.W. Baumann, A. Mishra, M.I. Worthley, A.J. Nelson, P.J. Psaltis, Management of multivessel coronary artery disease in patients with non-ST-elevation myocardial infarction: a complex path to precision medicine, *Ther Adv Chronic Dis* 11 (2020) 2040622320938527, <https://doi.org/10.1177/2040622320938527>.
- [17] S.B. Puchner, T. Liu, T. Mayrhofer, Q.A. Truong, H. Lee, J.L. Fleg, J.T. Nagurny, J.E. Udelsion, U. Hoffmann, M. Ferencik, High-risk plaque detected on coronary CT angiography predicts acute coronary syndromes independent of significant stenosis in acute chest pain: results from the ROMICAT-II trial, *J. Am. Coll. Cardiol.* 64 (2014) 684–692, <https://doi.org/10.1016/j.jacc.2014.05.039>.
- [18] Z.Q. Wang, Y.J. Zhou, Y.X. Zhao, D.M. Shi, Y.Y. Liu, W. Liu, X.L. Liu, Y.P. Li, Diagnostic accuracy of a deep learning approach to calculate FFR from coronary CT angiography, *J Geriatr Cardiol* 16 (2019) 42–48, <https://doi.org/10.11909/j.issn.1671-5411.2019.01.010>.
- [19] R.M. Jacoby, R.W. Nesto, Acute myocardial infarction in the diabetic patient: pathophysiology, clinical course and prognosis, *J. Am. Coll. Cardiol.* 20 (1992) 736–744.
- [20] J.B. Muhlestein, D.L. Lappe, J.A. Lima, B.D. Rosen, H.T. May, S. Knight, D.A. Bluemke, S.R. Towner, V. Le, T.L. Bair, A.L. Vavere, J.L. Anderson, Effect of screening for coronary artery disease using CT angiography on mortality and cardiac events in high-risk patients with diabetes: the FACTOR-64 randomized clinical trial, *JAMA* 312 (2014) 2234–2243, <https://doi.org/10.1001/jama.2014.15825>.
- [21] P. Raggi, Screening for atherosclerotic cardiovascular disease in patients with type 2 diabetes mellitus: controversies and guidelines, *Can. J. Diabetes* 44 (2020) 86–92, <https://doi.org/10.1016/j.jcjd.2019.08.009>.
- [22] K. Takamura, T. Kondo, S. Fujimoto, M. Hiki, R. Matsumori, Y. Kawaguchi, M. Amanuma, S. Takase, H. Daida, Incremental predictive value for obstructive coronary artery disease by combination of Duke Clinical Score and Agatston score, *Eur Heart J Cardiovasc Imaging* 17 (2016) 550–556, <https://doi.org/10.1093/ehjci/jev233>.
- [23] T.C. Villines, A.J. Taylor, Multi-ethnic study of atherosclerosis arterial age versus framingham 10-year or lifetime cardiovascular risk, *Am. J. Cardiol.* 110 (2012) 1627–1630, <https://doi.org/10.1016/j.amjcard.2012.07.018>.
- [24] D. Eng, C. Chute, N. Khandwala, P. Rajpurkar, J. Long, S. Shleifer, M.H. Khalaf, A.T. Sandhu, F. Rodriguez, D.J. Maron, S. Seyyedi, D. Marin, I. Golub, M. Budoff, F. Kitamura, M.S. Takahashi, R.W. Filice, R. Shah, J. Mongan, K. Kallianos, C.P. Langlotz, M.P. Lungren, A.Y. Ng, B.N. Patel, Automated coronary calcium scoring using deep learning with multicenter external validation, *NPJ Digit Med* 4 (2021) 88, <https://doi.org/10.1038/s41746-021-00460-1>.
- [25] S.J. Al'Aref, G. Maliakal, G. Singh, A.R. van Rosendaal, X. Ma, Z. Xu, O.A.H. Alawamlh, B. Lee, M. Pandey, S. Achenbach, M.H. Al-Mallah, D. Andreini, J.J. Bax, D.S. Berman, M.J. Budoff, F. Cademartiri, T.Q. Callister, H.J. Chang, K. Chinnaiyan, B.J.W. Chow, R.C. Cury, A. DeLago, G. Feuchtnr, M. Hadamitzky, J. Hausleiter, P.A. Kaufmann, Y.J. Kim, J.A. Leipsic, E. Maffei, H. Marques, P.A. Goncalves, G. Pontone, G.L. Raff, R. Rubinshtein, T.C. Villines, H. Gransar, Y. Lu, E.C. Jones, J.M. Pena, F.Y. Lin, J.K. Min, L.J. Shaw, Machine learning of clinical variables and coronary artery calcium scoring for the prediction of obstructive coronary artery disease on coronary computed tomography angiography: analysis from the CONFIRM registry, *Eur. Heart J.* 41 (2020) 359–367, <https://doi.org/10.1093/eurheartj/ehz565>.
- [26] D. Han, A. Lin, H. Gransar, D. Dey, D.S. Berman, Influence of coronary artery calcium score on computed tomography-derived fractional flow reserve: a meta-analysis, *JACC Cardiovasc Imaging* 14 (2021) 702–703, <https://doi.org/10.1016/j.jcmg.2020.09.022>.
- [27] H.J. Koo, J.W. Kang, S.J. Kang, J. Kweon, J.G. Lee, J.M. Ahn, D.W. Park, S.W. Lee, C.W. Lee, S.W. Park, S.J. Park, Y.H. Kim, D.H. Yang, Impact of coronary calcium score and lesion characteristics on the diagnostic performance of machine-learning-based computed tomography-derived fractional flow reserve, *Eur Heart J Cardiovasc Imaging* 22 (2021) 998–1006, <https://doi.org/10.1093/ehjci/jeab062>.
- [28] H. Mickley, K.T. Veien, O. Gerke, J. Lambrechtsen, A. Rohold, F.H. Steffensen, M. Husic, D. Akkan, M. Busk, L.B. Jessen, L.O. Jensen, A. Diederichsen, K. A. Ovrehus, Diagnostic and clinical value of FFR(CT) in stable chest pain patients with extensive coronary calcification: the FACC study, *JACC Cardiovasc Imaging* 15 (2022) 1046–1058, <https://doi.org/10.1016/j.jcmg.2021.12.010>.
- [29] A. Andreadi, S. Muscoli, R. Tajmir, M. Meloni, C. Muscoli, S. Ilari, V. Mollace, D. Della Morte, A. Bellia, N. Di Daniele, M. Tesaro, D. Lauro, Recent pharmacological options in type 2 diabetes and synergic mechanism in cardiovascular disease, *Int. J. Mol. Sci.* 24 (2023), <https://doi.org/10.3390/ijms24021646>.